CHAPTER 7

ANALYTICAL PROPERTIES OF SEMI-STATIONARY SUBDIVISION SCHEMES

Hongxin Zhang and Guojin Wang
State Key Laboratory of CAD&CG, Zhejiang University, Hangzhou, China
E-mail: zhx@cad.zju.edu.cn

Based on the viewpoint of topological and geometrical operators, we propose a novel class of subdivision schemes named semi-stationary subdivision for freeform surface design. Compared with traditional stationary methods, their main advantage lies in the use of a parameter changing rule during the subdivision iterations. This facilitates shape control by the user. Local revolving surfaces, directional and bumpy effects can be generated. For practical and theoretical importance, we strictly analyze the convergence properties of cubic subdivision schemes by employing Discrete Fourier Transform and matrix computing techniques to deal with the dynamic subdivision matrix. Additionally, we generalize its basic algorithms by selecting multi-kernel functions. The resulting surfaces are similar to Catmull-Clark subdivision surfaces and have G^2 continuity except at irregular points. The simplicity in mathematical theory and practical implementation further enhance the usefulness of these schemes in computer aided design and computer graphics.

1. Introduction

In an earlier paper,[12] we presented a novel class of discrete curve/surface construction schemes as an extension of stationary subdivision methods.[2,4] In these new schemes, subdivision stencils are modified regularly during the subdivision operations to generate special surfaces. The main purposes of this chapter are to analyze the convergence properties of the derived high-order subdivision surfaces and to offer several practical extensions.

We will first describe the semi-stationary schemes in Section 2. Section 3 presents the convergence analysis of the basic algorithm. The algorithmic generalizations, and several typical examples are shown in Section 4. Finally, conclusions are offered in Section 5.

2. Semi-stationary Schemes

About twenty years ago, Catmull and Clark introduced the first subdivision surface method.[2] This method is applied on an arbitrary space polyhedron, also called *control mesh*, denoted by M^0. By splitting every face of the control mesh into a group of quadrilateral sub-faces, the first level mesh M^1 is obtained. Specifically, an n-side face is divided into n spatial quadrangles. The positions of the vertices on the mesh M^1 are computed by some weight-averaging method. This procedure is called subdivision. The subdivision procedure is repeated to obtain finer and finer meshes, and the *subdivision surface* is defined as the limit of the mesh sequence $M^0, M^1, M^2, \ldots$. With appropriate averaging method (or stencil, mask), the subdivision surface can achieve certain order of continuity. The early schemes[2,4,6] use the same mask in every subdivision step; thus they are called *stationary subdivision schemes*.

In one of our former papers,[12] we have presented a non-stationary scheme. The main idea is to decompose the subdivision procedure into a combination of basic subdivision operators and a subsequence of neighborhood convolutions. We first define some operations over a given mesh M.

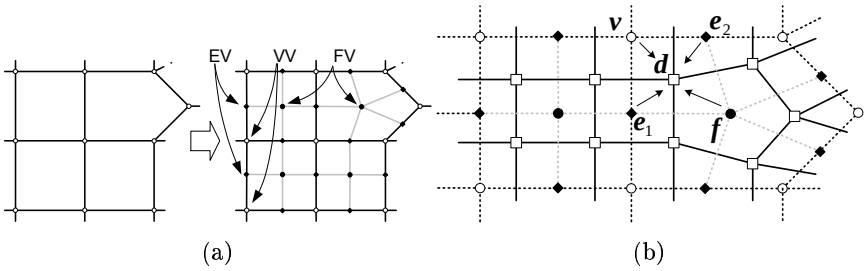

Fig. 1. Operations over mesh: (a) is the up-sampling operation, and (b) is the dual convolution.

Definition 1: (Up-sampling). Let M be a mesh. For each edge E in M we insert an edge-vertex (abbreviate as EV):

$$\mathbf{e}' = \frac{1}{2}(\mathbf{v}_1 + \mathbf{v}_2),$$

where $\mathbf{v}_1$ and $\mathbf{v}_2$ are the two end points of edge E. For each face F in M,

we create a new face-vertex (abbreviate as FV) on its central

$$\mathbf{f}' = \frac{1}{|F|} \sum_{\mathbf{v}_i \in F} \mathbf{v}_i.$$

Corresponding to each vertex v in M, we define $\mathbf{v}' = \mathbf{v}$ as the new vertex-vertex (abbreviated as VV). By connecting VV to EV and EV to FV, we obtain a new mesh M'. We denote this up-sampling operation as $M' = UM$.

Definition 2: (Dual convolution). Let M be a mesh generated by up-sampling operation. For each face in M, if it is a quadrangle, then create a dual point as follows:

$$\mathbf{d} = \frac{f(\alpha)^2\mathbf{v} + f(\alpha)(\mathbf{e_1} + \mathbf{e_2}) + \mathbf{f}}{(1 + f(\alpha))^2}; \tag{1}$$

otherwise the dual point is defined by

$$\mathbf{d} = \frac{1}{|F|} \sum_{\mathbf{v}_i \in F} \mathbf{v}_i. \tag{2}$$

Here $f(\cdot)$ is the *kernel function* with parameter α. By connecting the dual points lying on adjacent faces, we obtain a dual mesh M' from the original mesh M. We denote this dual convolution operation as $M' = D(f, \alpha)M$.

Henceforth, we call a continuous function $f(\cdot)$ a *kernel function* if there exists a constant $c > 0$ such that

$$|f(\alpha) - f(\beta)| < c|\alpha - \beta|, \quad \forall \alpha, \beta \in [-\varepsilon, \varepsilon].$$

The simplest case is when $f(\cdot) \equiv 1$. In this case, equation (1) is equivalent to equation (2) with $n = 4$ and the dual convolution is just the dual averaging. Moreover, we do not need to know whether the vertices of the given input mesh are FV, EV or VV. Thus we denote $D(1, \cdot)$ as D_1 and relax the condition that the input mesh must be generated by up-sampling operation.

Definition 3: (Semi-stationary subdivision). The semi-stationary subdivision $S_n(f, \alpha)$ $(n \geq 2)$ is defined by

$$\begin{cases} S_2(f, \alpha) = D(f, \alpha)U, \\ S_n(f, \alpha) = D_1 S_{n-1}(f, \alpha) \quad (n > 2). \end{cases}$$

Thus we can obtain a generic class of subdivision algorithms by recursively applying $S_n(f, \alpha)$ over a mesh and letting $\alpha \leftarrow \alpha/2$ each time, i.e., $M^{j+1} = S_n(f, 2^{-j}\alpha)M^j$. Note that our schemes are equivalent to Zorin and Schröder's[13] when $f(\cdot) \equiv 1$. But in our basic subdivision operator S_2,

the weights are dynamically modified due to the properties of the kernel function $f(\cdot)$. Hence we call the derived rules *semi-stationary subdivision schemes*.

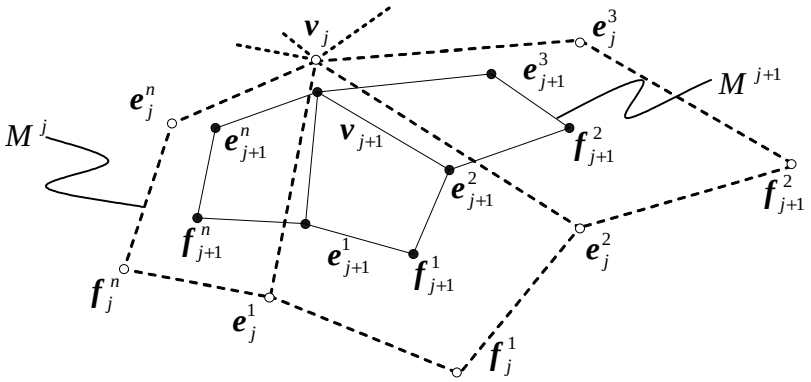

Fig. 2. Catmull-Clark subdivision: f, e and v are the face-vertices, edge-vertices and vertex-vertices respectively. The subscripts indicate the subdivision level, and the vertices around a vertex-vertex are marked with superscripts in counter-clockwise.

In a former work,[12] we have already defined and analyzed one special case $S_2(f,\alpha) = D(f,\alpha)U$. According to this framework, we can easily obtain an extended Catmull-Clark subdivision method by combining S_2 with one more step of dual convolution, i.e., $S_3(f,\alpha) = D_1 S_2(f,\alpha)$, which is also reported by Warren and others[7] when $f(\cdot) = \cos(\cdot)$. We construct the averaging masks as follows. As mentioned before, every vertex on M^{j+1} corresponds to a topological element which may be a face, an edge or a vertex on M^j; thus they are called face-vertex, edge-vertex and vertex-vertex respectively. In Fig. 2, $\mathbf{f}_j^i, \mathbf{e}_j^i, \mathbf{v}_j^i$ are face-vertex, edge-vertex and vertex-vertex respectively, where the subscript j represents the subdivision mesh level. With simple computations, one can check that FV is the averaging of the corresponding face vertices, i.e.,

$$\mathbf{f}_{j+1}^i = (\mathbf{v}_j + \mathbf{e}_j^i + \mathbf{f}_j^i + \mathbf{e}_j^{i+1})/4. \tag{3}$$

The equation of edge-vertex is

$$\mathbf{e}_{j+1}^i = \mu_j(\mathbf{v}_j + \mathbf{e}_j^i) + \nu_j(\mathbf{e}_j^{i-1} + \mathbf{f}_j^{i-1} + \mathbf{f}_j^i + \mathbf{e}_j^{i+1}), \tag{4}$$

where the superscript $i \in Z_n$, $Z_n := Z \bmod n$, and n is the vertex valence which is equal to the number of connected edges. The new vertex-vertex

equation is

$$\mathbf{v}_{j+1} = (1 - \beta_j - \gamma_j)\mathbf{v}_j + \frac{\beta_j}{n}\sum \mathbf{e}_j^i + \frac{\gamma_j}{n}\sum \mathbf{f}_j^i.$$

Here the accessorial coefficients are

$$\begin{cases} f_j = f(2^{-j-1}\alpha), \\ \mu_j = \dfrac{2f_j + 1}{4f_j + 4}, \qquad \nu_j = \dfrac{1}{8f_j + 8}, \\ \eta_j = \dfrac{(2f_j + 1)^2}{(2f_j + 2)^2}, \quad \xi_j = \dfrac{4f_j + 2}{(4f_j + 4)^2}, \quad \zeta_j = \dfrac{1}{(4f_j + 4)^2}, \\ \beta_j = 4\xi_j, \qquad \gamma_j = 4\zeta_j. \end{cases} \tag{5}$$

The vertices with valence 4 are called *regular vertices*, since its local area properties are the same as tensor product spline surface. Otherwise, they are *irregular vertices*.

3. Convergent and Continuity Analysis

In this section, we mainly discuss the convergence properties of the S_3 subdivision case around irregular vertices. This is because in the neighborhood of regular vertices, the generated surfaces by S_3 have similar properties as tensor product cubic spline. That is, the surface continuity in regular cases can be derived from the continuity of the corresponding curve subdivision method (please refer, e.g., to our former papers[11,12] for details). In an earlier work of Dyn and Levin,[5] they proved for curves that if a non-stationary scheme mask converges to the stationary mask sufficiently fast, then the non-stationary curve has the same continuity properties as the stationary scheme. Then applying Theorem 8 in their paper, our S_2 curve case is C^1 when the sufficient condition $f(0) > 1/2$ for the kernel function $f(.,.)$ is satisfied.[12] Since the subsequence subdivision curve scheme S_n is obtained by combining the convolution operator $n-2$ times, they can achieve C^{n-1}. Thus, as a special case, the S_3 surface scheme is C^2 continuous except at irregular vertices.

3.1. *Local Subdivision Structure*

After one step of subdivision, all faces in the new mesh are quadrangles and the number of irregular vertices is fixed. If we subdivide the mesh further, irregular vertices will be isolated; in other words, each face contains at most one irregular vertex. In the following subdivision surface analysis, we

shall assume that we have done sufficient steps of subdivision to generate the local subdivision structure shown in Fig. 3. The vertex marked as 0 is an irregular vertex with valence n. Its neighborhood is separated by incident edges into n sub-regions, which are called *segments* and are marked in counterclockwise order. In each segment, from center to outside, the control vertices are also numbered in counterclockwise order. After j times subdivision, we denote the vertex sequence around the irregular vertex as $\mathbf{P}_j := [\mathbf{P}_j^0; \mathbf{P}_j^1; \ldots; \mathbf{P}_j^{n-1}]^{\mathrm{T}}$, where $\mathbf{P}_j^k := [\mathbf{P}_j^{k,0}, \mathbf{P}_j^{k,1}, \ldots, \mathbf{P}_j^{k,m-1}]^{\mathrm{T}}$ is the vertex sub-sequence in segment k with $m = L(L+1)+1$ for L-level neighborhood. For convenience, we also define $\mathbf{O}_j := \mathbf{P}_j^{0,0} = \mathbf{P}_j^{1,0} \cdots = \mathbf{P}_j^{n-1,0}$. To analyze the first order continuity, we consider the 3-level vertex neighborhood of the irregular vertex, i.e., $m = 13$.

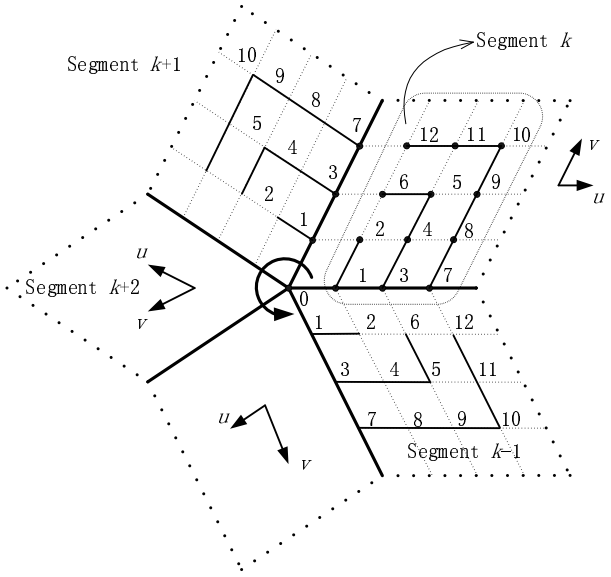

Fig. 3. Local subdivision structure

3.2. *Subdivision Matrix*

Based on the subdivision schemes described in the last section, two successive vertex sequences have the following relationship

$$\mathbf{P}_j = \mathbf{S}_j \mathbf{P}_{j-1}.$$

Here $\mathbf{S}_j$ is an $mn \times mn$ matrix related to the subdivision level index j. Obeying the former segmented control vertices coding rules, the subdivision matrix $\mathbf{S}_j$ is made up of $n \times n$ matrix blocks $\mathbf{S}_j^{i,i'}$ whose size is $m \times m$. Thus we have

$$\mathbf{P}_j^k = \sum_{i=0}^{n-1} \mathbf{S}_j^{k,i} \mathbf{P}_{j-1}^i, \quad k \in Z_n. \tag{6}$$

The subdivision matrix has the following properties:

1. the sum of elements of each row is equal to 1;
2. the cyclic symmetry:

$$\mathbf{S}_j^i := \mathbf{S}_j^{i,0} = \mathbf{S}_j^{i+i',i'}, \quad i, i' \in Z_n.$$

By property 2, equation (6) can be re-written as

$$\mathbf{P}_j^k = \sum_{i=0}^{n-1} \mathbf{S}_j^{k-i} \mathbf{P}_{j-1}^i, \quad k \in Z_n.$$

Furthermore, noting property 2, we introduce the DFT (Discrete Fourier Transform):

$$\tilde{x}^k := \sum_{i=0}^{n-1} \omega_n^{-ik} x^i, \quad k \in Z_n.$$

Here $\omega_n := c_n + i s_n = \exp(2\pi i/n)$, and $x = (x^0, x^1, \ldots, x^{n-1})$ is an n-tuple whose elements can be scale value, vector or matrix. Applying DFT on both sides of equation (6), we obtain

$$\mathbf{S}_j = \mathbf{W} \mathrm{diag}(\tilde{\mathbf{S}}_j^0, \tilde{\mathbf{S}}_j^1, \ldots, \tilde{\mathbf{S}}_j^{n-1}) \mathbf{W}^{-1}, \tag{7}$$

with $\mathbf{W} = (\mathbf{W}_{ij})_{n \times n}, \mathbf{W}_{ij} = \omega_n^{ij} \mathbf{I}_{m \times m}$, $i, j \in \{0, 1, ..., n-1\}$. After several computations, one finds that the $m \times m$ matrix blocks $\tilde{\mathbf{S}}_j^k$ have the following structure

$$\tilde{\mathbf{S}}_j^k = \begin{pmatrix} \mathbf{A}_j^k & 0 & 0 \\ \mathbf{A}_{1,0}^k & \mathbf{B}_j^k & 0 \\ \mathbf{A}_{2,0}^k & \mathbf{A}_{2,1}^k & 0 \end{pmatrix},$$

where the sub-matrices in the diagonal line are

$$\mathbf{A}_j^k = \begin{pmatrix} (1 - \beta_j - \gamma_j)\delta_{k,0} & \beta_j & \gamma_j \\ \nu \delta_{k,0} & 2\mu_j c_n + \nu_j & \nu_j(1 + \bar{\omega}_n^k) \\ \frac{1}{4}\delta_{k,0} & \frac{1}{4}(1 + \omega_n^k) & \frac{1}{4} \end{pmatrix}$$

and

$$\mathbf{B}_j^k = \begin{pmatrix} \xi_j & \zeta_j & 0 & \zeta_j\bar{\omega}_n^k \\ \nu_j & \nu_j & 0 & 0 \\ \zeta_j(1+\omega_n^k) & \xi_j & \zeta_j & \xi_j \\ \nu_j\omega_n^k & 0 & 0 & \nu_j \end{pmatrix}.$$

In the last two equations, $\delta_{i,j}$ is the Kronecker delta. The eigenvalues of the sub-matrix $\mathbf{B}_j^k$ is

$$\left\{\tau_j^{k,1}, \tau_j^{k,2}, \tau_j^{k,3}, \tau_j^{k,4}\right\} = \left\{\frac{1}{16(1+f_j)^2}, \frac{f_j}{8(1+f_j)^2}, \frac{1}{8(1+f_j)}, \frac{1}{4(1+f_j)}\right\}. \tag{8}$$

When $f_j > 0$, the four eigenvalues are all less than $1/4$. For sub-matrix $\mathbf{A}_j^k$, if $k = 0$, and let $\sigma_j = 1 - \beta_j - \gamma_j$, its three eigenvalues are 1 and

$$\lambda_j^{0,i} = \frac{1}{8}\left(4\sigma_j - 1 \pm \sqrt{(4\sigma_j - 1)^2 + 8(2\beta_j - 1)\frac{f_j}{1+f_j}}\right), \quad i = 1, 2.$$

By equation (5), we can obtain $\lambda_j^{0,1} = {f_j}^2(2+2f_j)^{-2} < 1/4$ and $\lambda_j^{0,2} = f_j(2+2f_j)^{-1} < 1/2$. If $k \neq 0$, then the two none-zero eigenvalues are

$$\lambda_j^{k,i} = \frac{1}{8(1+f_j)}\left(c_{n,k} + 2 + 3f_j \pm \sqrt{c_{n,k}^2 + c_{n,k}(4+6f_j) + (2+f_j)^2}\right), \quad i = 1, 2,$$

with $c_{n,k} = \cos(2\pi k/n)$. Denote

$$\begin{aligned} \lambda_j &:= \lambda_j^{1,1} = \lambda_j^{n-1,1} \\ &= \frac{1}{8(1+f_j)}\left(c_n + 2 + 3f_j + \sqrt{c_n^2 + c_n(4+6f_j) + (2+f_j)^2}\right); \end{aligned}$$

we can get $1 > \lambda_j \geq 1/2 > \lambda_j^{k,2} > 0$ $(k = 1, 2, \ldots, n-1)$ and $\lambda_j > \lambda_j^{k,1} > 1/8$ $(k = 2, 3, \ldots, n-2)$ for every n.

3.3. *Convergence of Semi-stationary Subdivision Schemes*

We analyze the convergence of semi-stationary subdivision schemes in this subsection. Denote $\mathbf{T}_j = \mathbf{S}_j\mathbf{S}_{j-1}\cdots\mathbf{S}_1$ and $\tilde{\mathbf{T}}_j^k = \tilde{\mathbf{S}}_j^k\tilde{\mathbf{S}}_{j-1}^k\cdots\tilde{\mathbf{S}}_1^k$. By equa-

tion (7), we have

$$\begin{aligned}\mathbf{P}_j &= \mathbf{S}_j\mathbf{P}_{j-1}\\ &= \cdots\\ &= \mathbf{S}_j\mathbf{S}_{j-1}\cdots\mathbf{S}_1\mathbf{P}_0\\ &= \mathbf{T}_j\mathbf{P}_0\\ &= \mathbf{W}\mathrm{diag}(\tilde{\mathbf{T}}_j^0,\tilde{\mathbf{T}}_j^1,\ldots\tilde{\mathbf{T}}_j^{n-1})\mathbf{W}^{-1}\mathbf{P}_0.\end{aligned} \tag{9}$$

By induction, we can conclude that the sum of each row of $\mathbf{T}_j$ is equal to 1. Thus $(1,1,\ldots,1)^T$ must be its eigenvector corresponding to the largest eigenvalue 1. Thus, we obtain the following theorem.

Theorem 4: If $f_j > 0$ $(j = 1,2,\ldots)$, the spectrum radius of matrix $\mathbf{T}_j$ is equal to the largest eigenvalue 1, and the other eigenvalues will be convergent to 0 when $j \to \infty$, then the subdivision schemes are convergent and continuous.

Proof: If $f_j > 0$ $(j = 1,2,\ldots)$, then the elements of $\mathbf{T}_j$ are non-negative. In other words, the transpose of $\mathbf{T}_j$ is a stochastic matrix, so the spectrum radius of $\mathbf{T}_j$ is 1. By equation (9), the eigenvalues of $\mathbf{T}_j$ are the same as the blocked diagonal matrix $\mathrm{diag}(\tilde{\mathbf{T}}_j^0,\ldots,\tilde{\mathbf{T}}_j^{n-1})$. Based on the analysis in the last section, one can show that for every j, when $k \neq 0$, there exists a positive real number c such that the spectrum norm of $\tilde{\mathbf{S}}_j^k$ satisfies $\|\tilde{\mathbf{S}}_j^k\|_2 < c < 1$. By the matrix norm properties, we have

$$\left\|\tilde{\mathbf{T}}_j^k\right\| \leq \left\|\tilde{\mathbf{S}}_j^k\right\|\left\|\tilde{\mathbf{S}}_{j-1}^k\right\|\cdots\left\|\tilde{\mathbf{S}}_1^k\right\| < c^j.$$

So, when $j \to \infty$, $\|\tilde{\mathbf{T}}_j^k\| \to 0$. It follows that the eigenvalues of $\tilde{\mathbf{T}}_j^k$ $(k \neq 0)$ are all convergent to 0.

When $k = 0$, from the last section, we know that all eigenvalues of $\mathbf{B}_j^0$ are less than $1/4$. Similarly, one can verify that all eigenvalues of $\mathbf{B}_j^0\mathbf{B}_{j-1}^0\cdots\mathbf{B}_1^0$ are convergent to 0. For $\tilde{\mathbf{S}}_j^0$'s sub-block $\mathbf{A}_j^0$, its Jordan decomposition is $\mathbf{A}_j^0 = \mathbf{V}_j\mathrm{diag}(1,\lambda_1^0,\lambda_2^0)\mathbf{V}_j^{-1}$ with

$$\mathbf{V}_j = \begin{pmatrix} 1 & (1+f_j)^{-2} & -(1+f_j)^{-1} \\ 1 & -(1+f_j)^{-1} & (2+2f_j)^{-1} \\ 1 & 1 & 1 \end{pmatrix},$$

and

$$\mathbf{V}_{j+1}^{-1}\mathbf{V}_j = \begin{pmatrix} 1 & \frac{(f_j - f_{j+1})^2}{(1+f_j)^2(2+f_{j+1})^2} & \frac{f_j - f_{j+1}}{(1+f_j)(2+f_{j+1})} \\ 0 & \frac{(2+f_j)^2(1+f_{j+1})^2}{(1+f_j)^2(2+f_{j+1})^2} & 0 \\ 0 & \frac{2(2+f_j)(f_j - f_{j+1})(1+f_{j+1})}{(1+f_j)^2(2+f_{j+1})^2} & \frac{(2+f_j)(1+f_{j+1})}{(1+f_j)(2+f_{j+1})} \end{pmatrix}.$$

Thus, the eigenvalues of $\mathbf{A}_j^0\mathbf{A}_{j-1}^0 \ldots \mathbf{A}_1^0$ are convergent to $(1,0,0)$ with $j \to \infty$. So there is a $\mathbf{T}_\infty$ which is the limit of $\mathbf{T}_j$ and whose eigenvalues are $(1,0,\ldots,0)$. Since $\mathbf{T}_\infty = \mathbf{R}_1 \mathrm{diag}(1,0,...,0)\mathbf{R}_2$, we have $\mathrm{rank}(\mathbf{T}_\infty) = 1$. Furthermore, it follows that there exists an $n \times m$-dimensional vector $\mathbf{a} = [a_1, a_2, \ldots, a_{mn}]$ such that $\mathbf{T}_\infty = [\mathbf{a}, \mathbf{a}, \ldots, \mathbf{a}]^{\mathrm{T}}$ and $\mathbf{P}_\infty = \mathbf{T}_\infty \mathbf{P}_0$. Hence the subdivision schemes are convergent. □

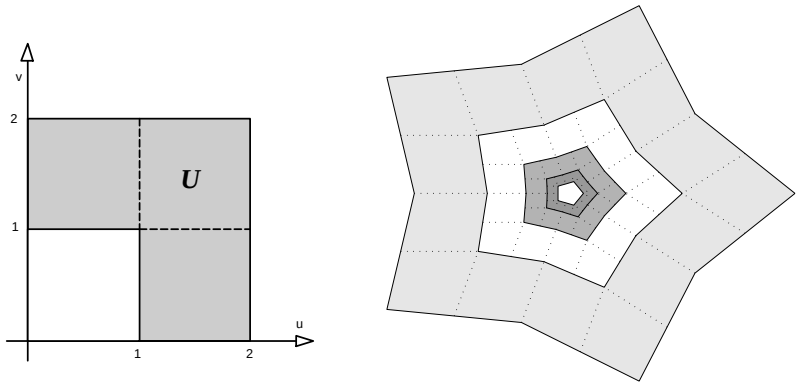

(a) Parametric domain (b) Ring surface layers

Fig. 4. The strict convergence definitions of subdivision surface

3.4. *Continuity of Semi-stationary Subdivision Surface*

In the continuity analysis of stationary subdivision surfaces,[1,9,8] the tangent plane continuity around an irregular vertex is defined by the limit of the tangent plane of the tensor product patch. Similarly, we strictly define the continuity of semi-stationary subdivision surfaces as follows. On a mesh, surrounding a single irregular vertex, the regular part of the control

polygon corresponds to the tensor product surface $\mathbf{y}_j$ defined by the corresponding curve subdivision scheme.[12] By applying the subdivision operator, it produces an ascending surface sequence

$$\mathbf{y}_0 \subset \mathbf{y}_1 \subset \mathbf{y}_2 \subset \cdots$$

which converges to the limit surface $\mathbf{y} = \bigcup_{i=1}^{\infty} \mathbf{y}_i$. Then we introduce the ring surface layers

$$\mathbf{r}_j := \text{closure}(\mathbf{y}_{j+1} \backslash \mathbf{y}_j).$$

So we can define the limit surface as the union of non-intersected sets

$$\mathbf{y} = (\bigcup_{j \in N} \mathbf{r}_j) \cup \mathbf{y}_0.$$

Thus $\mathbf{r}_j$ are just defined on the parameter area $U \times Z_n$, with $U := [0,2]^2 \backslash [0,1]^2$. And every layer $\mathbf{r}_j$ can be represented as a linear combination of piecewise continuous functions N^k with control points $\mathbf{P}_j^k$, i.e.,

$$\mathbf{r}_j : \quad (u,v,k) \in U \times Z_n \mapsto \mathbf{r}_j^k(u,v) = \sum_{l=0}^{L} N^l(u,v,k)\mathbf{P}_j^l.$$

Furthermore, all the N^l can be represented as a row vector $\mathbf{N}$ and the control points $\mathbf{P}_j^k$ form a column vector $\mathbf{P}_j$. Then we have the following matrix form

$$\mathbf{r}_j(u,v,k) = \mathbf{r}_j^k(u,v) = \mathbf{N}(u,v,k)\mathbf{P}_j.$$

So we can more strictly give the convergence definition of subdivision surfaces (see Fig. 4).

Definition 5: A subdivision procedure S is *convergent*, if there exists a unique point $\mathbf{p}$ such that for any point sequence $\mathbf{p}_j \in \mathbf{r}_j$,

$$\lim_{j \to \infty} \mathbf{p}_j = \mathbf{p}.$$

Since $\mathbf{r}_j(u_0, v_0)$ is the convex linear combination of control points, the method we used to prove the control points convergent in Theorem 4 is equivalent to Definition 5. Note that the surface defined by Definition 5 is also continuous. We introduce the tangent plane continuity as follows.

Definition 6: A subdivision procedure S is *tangent plane continuous*, if S is convergent, and there exists a unique vector $\mathbf{n}(\mathbf{p})$ such that for any normal vector sequence $\mathbf{n}(\mathbf{p}_j)$, $\mathbf{p}_j \in \mathbf{r}_j$,

$$\lim_{j \to \infty} \mathbf{n}(\mathbf{p}_j) = \mathbf{n}(\mathbf{p}).$$

The vector $\mathbf{n}(\mathbf{p})$ is called the subdivision surface normal limit at $\mathbf{p}$.

Note that it is not necessary to be the true normal at $\mathbf{p}$, since it may not exist. Obeying the former definitions, we can prove the following theorem.

Theorem 7: If $f(0) \geq 1$, then the subdivision surfaces defined by scheme S_3 are tangent plane continuous.

Proof: By the definition, let $\mathbf{p}_j$ be an arbitrary point on the j-th layer ring surface with correspond parameters (u_0, v_0, k_0), and its normal vector is $\mathbf{n}(\mathbf{p}_j)$ which is paralleled to $\mathbf{r}_u^j \times \mathbf{r}_v^j \big|_{(u_0,v_0,k_0)}$. Obviously, there is an $mn \times mn$ matrix D_u^j such that $\mathbf{r}_x^j = \mathbf{D}_x^j \mathbf{P}_j = \mathbf{D}_x^j \mathbf{T}_j \mathbf{P}_0$ with $x \in \{u, v\}$. By the analyze in Subsections 3.2 and 3.3, $\mathbf{T}_j$ has the eigen-structure $(\mathbf{V}_j, \Delta_j)$ in the complex domain such that there exists a diagonal decomposition $\mathbf{T}_j = \mathbf{V}_j \Delta_j \mathbf{V}_j^{-1}$ with $\mathbf{V}_j = (\mathbf{v}_j^1, \mathbf{v}_j^2, \ldots, \mathbf{v}_j^{mn})$ and $\Delta_j = \mathrm{diag}(1, \delta_2^j, \ldots, \delta_{mn}^j)$. Here $\mathbf{v}_j^k$ are $m \times n$-dimension vectors, and we assume that

$$1 > \left|\delta_2^j\right| \geq \left|\delta_3^j\right| \geq \ldots \geq \left|\delta_{mn}^j\right|, \quad \mathbf{v}_j^1 = 1/\sqrt{mn}(1, 1, \ldots, 1).$$

Denote

$$\mathbf{Q}_j := \mathbf{V}_j^{-1} \mathbf{P}_0 := (\mathbf{Q}_j^1, \mathbf{Q}_j^2, \ldots, \mathbf{Q}_j^{mn});$$

we have

$$\mathbf{x}_u^j \times \mathbf{x}_v^j = \sum_{k=1}^{mn-1} \sum_{l=k+1}^{mn} \delta_j^k \delta_j^l \left[(\mathbf{D}_u^j \mathbf{v}_j^k)(\mathbf{D}_v^j \mathbf{v}_j^l) - (\mathbf{D}_u^j \mathbf{v}_j^l)(\mathbf{D}_v^j \mathbf{v}_j^k) \right] \mathbf{Q}_j^k \times \mathbf{Q}_j^l.$$

Note that the subdivision schemes we have defined are all linear precision. So, the sum of each row elements of D_x^x are 0 and $D_x^j \mathbf{v}_j^1 = 0$. From the last theorem and because of the symmetry properties of $\mathbf{T}_j$, diagonalizing it with DFT, we see that all eigenvalues of $\mathbf{T}_j$ except 1 are convergent to 0. But the convergent speeds of different eigenvalues are different. By Lemmas A.1 and A.2, δ_j^2 and δ_j^3 are generated from the matrix blocks $\mathbf{A}_j^1$ and $\mathbf{A}_j^{n-1}$, and

$$\lim_{j \to \infty} \delta_j^k / \delta_j^2 = \begin{cases} 0, & k \neq 3, \\ c, & k = 3. \end{cases}$$

Furthermore, the limits of $\mathbf{Q}_j^2$ and $\mathbf{Q}_j^3$ exist. It follows that

$$\lim_{j \to \infty} \mathbf{n}(\mathbf{p}_j) = \lim_{j \to \infty} \mathbf{x}_u^j \times \mathbf{x}_v^j / \left\| \mathbf{x}_u^j \times \mathbf{x}_v^j \right\| = \mathbf{Q}_\infty^2 \times \mathbf{Q}_\infty^3 / \left\| \mathbf{Q}_\infty^2 \times \mathbf{Q}_\infty^3 \right\|.$$

By the definition, the subdivision schemes can reach tangent plane continuity. □

Remark 8: Reif[9] pointed out that it is not enough to only check the normal vector convergence for tangent plane continuity. He proved that if the characteristic map of a given stationary subdivision scheme is regular and injective, then it is G^1 at an irregular vertex. However, it is impossible in our semi-stationary case to directly define a characteristic map via the dynamic subdivision matrices. Fortunately, in the proof of Theorem 7, $\mathbf{Q}_\infty^i$ $(i = 2, 3)$ exist, which correspond to the eigenvectors in the stationary case to define the characteristic map. Note that $\mathbf{Q}_\infty^i$ can be viewed as continuous vector functions with subdivision parameter α, and $\alpha \equiv 0$ defines the stationary case, which is well researched by Reif[9] and Zorin.[13] So we conclude that at irregular vertices the S_3 scheme can achieve G^1.

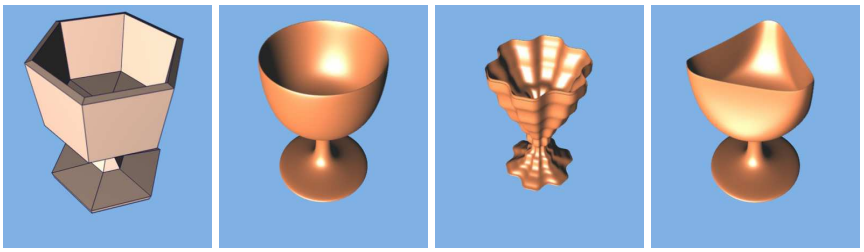

(a) (b) (c) (d)

Fig. 5. Examples of semi-subdivision surfaces with local revolving part: (a) is the original control mesh; (b) shows revolving result created by typical settings with $f(\cdot) = \cos(\cdot), \alpha = 2\pi/6$; (c) produces special effect with $f(\cdot) = \cos(\cdot), \alpha = 10$; (d) is an example of applying non-uniform parameter selection over the vertices. All the examples are generated based on S_3 schemes.

4. Examples with Discussions

In this section, we give several examples of surfaces generated by our subdivision schemes.

Revolving surfaces are very important in CAD/CAM. In our algorithmic framework, it is very easy to create subdivision surfaces with local revolving part. We can simply select $S_3(\cos, \alpha)$ as the subdivision scheme. In the revolving part, we construct several regular n-sided planar polygons along an axis and set $\alpha = 2\pi/n$. The results demonstrate that our technique can be an alternative solution for representing circular shape exactly, though it is also possible to use non-uniform rational subdivision techniques.[10] In our framework, we can also change the value of α to modify the shape, which

resembles rational-based techniques (see Fig. 5). To generate a complete surface of revolution, we apply the same method described by Morin and others[7] — use collapsed quads and alter the rules of linear subdivision $S_3(1,0)$ to generate exact surfaces of revolution. We wish to point out that it is not necessary for the whole mesh to use the same kernel function $f(\cdot)$ and parameter α. We have implemented a scheme with non-uniform parameters which can tag different α over a given mesh.

Some surfaces are anisotropic. For example, surfaces of revolution and sweeping can be viewed as a kind of anisotropic feature of surfaces. Furthermore, in the case of tensor product spline surfaces, one can choose different bases in different directions. However, traditional subdivision schemes are cyclic symmetric. Thus it is not powerful enough for certain geometric modelling applications. Researchers have employed the techniques of tagging special sharp features on meshes to enhance the classical stationary schemes.[3] Following these cues, we have developed a technique to create a directional fields over meshes by tagging the edges when applying semi-stationary subdivision schemes.[11] We call them longitude-latitude tags. Thus a new extension scheme can be easily obtained. The basic idea is to apply different kernel functions and α's along the longitude and latitude tagged edges (see Fig. 6).

5. Conclusion

We have presented a novel set of subdivision schemes in this chapter. Although they have dynamic subdivision matrices, we have shown that it is still possible to apply DFT-like techniques to analyze the geometric continuity properties. Compared with stationary schemes, our schemes are more flexible though less efficient. They can be used to create local revolving surfaces and anisotropic features. In the future, we will study the analytical properties of the anisotropic extended schemes.

Acknowledgements

We thank the reviewers for their comments which helped us to improve the content and the presentation of the chapter. Special thanks go to Professor Chiew-Lan Tai for her careful proof reading. This work is supported jointly by the National Natural Science Foundation of China (Grant No. 60173034), National Natural Science Foundation for Innovative Research Groups (No. 60021201) and the State Key Basic Research Project 973 (Grant No. 2002CB312101).

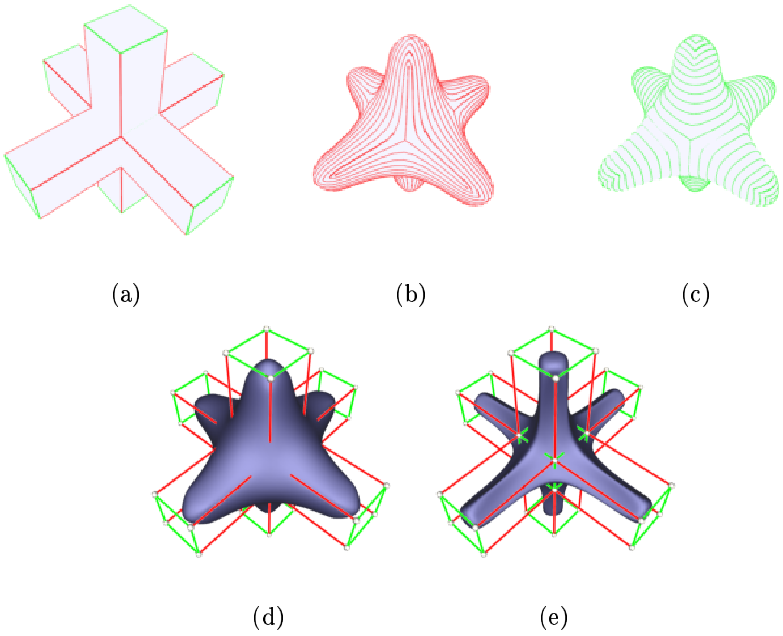

Fig. 6. Example of subdivision surfaces with anisotropic feature: (a) is the original control mesh with tags; (b) and (c) are the latitude and longitude tags respectively after three subdivision steps; (d) and (e) are two resulting surfaces by applying different kennel functions. Both examples are based on the extended S_3 schemes.

References

1. A. A. Ball and D. J. Storry. Conditions for tangent plane continuity over recursively generated B-spline surfaces. *ACM Transactions on Graphics*, 7(2): 83–102, 1988.
2. E. Catmull and J. Clark. Recursively generated B-spline surfaces on arbitrary topological meshes. *Computer Aided Design*, 10(6): 350–355, 1978.
3. T. DeRose, M. Kass, and T. Truong. Subdivision surfaces in character animation. *Computer Graphics*, 32 (Annual Conference Series): 85–94, 1998.
4. D. Doo and M. Sabin. Behavior of recursive division surfaces near extraordinary points. *Computer Aided Design*, 10(6): 356–360, 1978.
5. N. Dyn and D. Levin. Analysis of asymptotically equivalent binary subdivision schemes. *Journal of Mathematical Analysis and Applications*, 193(2): 594–621, 1995.
6. N. Dyn, D. Levin, and J. Gregory. A butterfly subdivision scheme for surface interpolation with tension control. *ACM Transactions on Graphics*, 9(2): 160–169, 1990.
7. G. Morin, J. Warren, and H. Weimer. A subdivision scheme for surfaces of revolution. *Computer Aided Geometric Design*, 18: 483–502, 2001.

8. J. Peters and U. Reif. Analysis of algorithms generalizing B-spline subdivision. *SIAM Journal of Numerical Annual*, 35: 728–748, 1998.
9. U. Reif. A unified approach to subdivision algorithms near extraordinary vertices. *Computer Aided Geometric Design*, 12(2): 153–174, 1995.
10. T. W. Sederberg, J. M. Zheng, D. Sewell, and M. Sabin. Non-uniform recursive subdivision surfaces. *Computer Graphics*, 32 (Annual Conference Series): 387–394, 1998.
11. H. X. Zhang and G. J. Wang. Semi-stationary push-back subdivision schemes. *Journal of Software*, 13(9): 1830–1839, 2002.
12. H. X. Zhang and G. J. Wang. Semi-stationary subdivision operators in geometric modeling. *Progress in Natural Science*, 12(10): 772–776, 2002.
13. D. Zorin and P. Schröder. A unified framework for primal/dual quadrilateral subdivision schemes. *Computer Aided Geometric Design*, 18: 429–454, 2001.

Appendix A. Proofs of the Two Lemmas

Lemma A.1: *Let* $\mathbf{K}_j^k = \frac{\mathbf{A}_j^k}{\lambda_j}\frac{\mathbf{A}_{j-1}^k}{\lambda_{j-1}}\cdots\frac{\mathbf{A}_1^k}{\lambda_1}$*; then:*

(*a*) *The eigenvalues of* $\mathbf{K}_j^0$ *except 1 are convergent to 0, when* $j \to \infty$.
(*b*) *If* $k \neq 0, 1, n-1$*, then the eigenvalues of* $\mathbf{K}_j^k$ *convergent to 0, when* $j \to \infty$.
(*c*) *If* $k = 1, n-1$*, then the matrix limit* $\lim_{j\to\infty} \mathbf{K}_j^k = \mathbf{K}_\infty^k$*, and* $\left\|\mathbf{K}_\infty^k\right\| > 0$ *when* $j \to \infty$*. In other words, they have a unique non-zero eigenvalue.*

Proof: Firstly, one can directly compute out all three eigenvalues of $\mathbf{K}_j^0$; they are

$$\left\{1, \frac{\lambda_j^{0,1}\lambda_{j-1}^{0,1}\cdots\lambda_1^{0,1}}{\lambda_j\lambda_{j-1}\cdots\lambda_1}, \frac{\lambda_j^{0,2}\lambda_{j-1}^{0,2}\cdots\lambda_1^{0,2}}{\lambda_j\lambda_{j-1}\cdots\lambda_1}\right\}.$$

This proves case (a).

When $k \neq 0, 1, n-1$, we have the following spectrum norm estimation

$$\left\|\mathbf{K}_j^k\right\| \leq \frac{\left\|\mathbf{A}_j^k\right\|\left\|\mathbf{A}_{j-1}^k\right\|\cdots\left\|\mathbf{A}_1^k\right\|}{\lambda_j\lambda_{j-1}\cdots\lambda_1} = \frac{\lambda_j^{k,1}\lambda_{j-1}^{k,1}\cdots\lambda_1^{k,1}}{\lambda_j\lambda_{j-1}\cdots\lambda_1}.$$

Then for a given scale M such that $\alpha \in [0, M)$, we have

$$\lim_{j\to\infty} \lambda_j^{k,1}/\lambda_j = \lambda_j^{k,1}(0)/\lambda_j(0) < 1,$$

where $\lambda_j^*(0)$ are the eigenvalues of $\mathbf{K}_j^k(0)$. It follows that $\left\|\mathbf{K}_j^k\right\| \to 0$ when $j \to \infty$. Thus case (b) is verified.

Note that $\mathbf{K}_j^k(\alpha)$ is determined by parameter α. When $k = 1$, we denote

$$\tilde{\mathbf{S}}_j^1(0) = \hat{\mathbf{S}}$$

and assume that the Jordan decomposition $\hat{\mathbf{S}} = \mathbf{Y}\Lambda\mathbf{Y}^{-1}$ exists. Consider

$$\Delta_j = \mathbf{V}^{-1}(\mathbf{S}_j^1(\alpha) - \mathbf{S}_j^1(0))\mathbf{V}.$$

When $\|\Delta_j\| \leq 2^{-j}C\alpha$, we have the following estimation

$$\begin{aligned}&\left\|\hat{\mathbf{S}}^j - \mathbf{S}_j^1(\alpha)\mathbf{S}_{j-1}^1(\alpha)\cdots\mathbf{S}_1^1(\alpha)\right\| \\ &\quad = \left\|\mathbf{Y}[\Lambda^j - (\Lambda+\Delta_j)(\Lambda+\Delta_{j-1})\cdots(\Lambda+\Delta_1)]\mathbf{Y}^{-1}\right\| \\ &\quad \leq C_1\alpha.\end{aligned}$$

Let $\lambda \triangleq \lambda_j(0) = \cdots = \lambda_1(0)$; it follows that

$$\lim_{j\to\infty} \lambda_j^1\lambda_{j-1}^1\cdots\lambda_1^1/\lambda^j = C_2 > 0.$$

So, there is a real number $C_3 > 0$ such that

$$\left\|\mathbf{K}_j^k(\alpha) - \mathbf{K}_j^k(0)\right\| \leq C_3\alpha.$$

Since the limit of sequence $\mathbf{K}_j^1(0) = \mathbf{Y}\mathrm{diag}(1, (\lambda_1^{1,2}(0)/\lambda)^j)\mathbf{Y}^{-1}$ is $\mathbf{K}_\infty^1(0)$, it follows that $\mathbf{K}_j^k(\alpha)$ is continuous near the zero point. Note that $\mathbf{K}_j^1(\alpha) = \mathbf{K}_{j-1}^1(\alpha/2)\tilde{\mathbf{S}}_1^1(\alpha)/\lambda_1(\alpha)$, so we can analyze the continuous property just in the neighborhood of the zero point. Furthermore, by the continuity, we have $\left\|\mathbf{K}_\infty^1(\alpha)\right\| \in (1-\varepsilon, 1+\varepsilon)$ with $\varepsilon > 0$, i.e., the largest eigenvalue is non-zero. For

$$\det(\mathbf{K}_j^1) = \det(\frac{\mathbf{S}_j^1\mathbf{S}_{j-1}^1\cdots\mathbf{S}_1^1}{\lambda_j\lambda_{j-1}\cdots\lambda_1}) = \frac{\lambda_j^{1,2}\lambda_{j-1}^{1,2}\cdots\lambda_1^{1,2}}{\lambda_j\lambda_{j-1}\cdots\lambda_1} \to 0$$

when $j \to \infty$, it is shown that other eigenvalues tend to zero. With a similar procedure, we can prove the case (c) when $k = n-1$. □

Lemma A.2: *Let* $\mathbf{L}_j^k = \frac{\mathbf{B}_j^k}{\lambda_j}\frac{\mathbf{B}_{j-1}^k}{\lambda_{j-1}}\cdots\frac{\mathbf{B}_1^k}{\lambda_1}$. *Then* $\mathbf{L}_j^k$ *tend to zero when* $j \to \infty$.

Proof: By direct calculation, one can verify that the eigen-vectors of $\mathbf{B}_j^k$ are

$$\begin{cases}\mathbf{b}_1 = \{0,0,1,0\}, \\ \mathbf{b}_2 = \{-\frac{1}{\omega(1+f_j)}, \omega^{-1}, -\frac{(1+6f_j+4f_j^2)(1+\omega)}{(1-f_j-2f_j^2)\omega}, 1\}, \\ \mathbf{b}_3 = \{0, -\omega^{-1}, 2(1-\omega^{-1}), 1\}, \\ \mathbf{b}_4 = \{\omega^{-1}, \omega^{-1}, 1+\omega^{-1}, 1\}.\end{cases}$$

Denote $t_i = \tau_j^{k,i}\cdots\tau_1^{k,i}$ and $\mathbf{B}(j,k) = \mathbf{B}_j^k\mathbf{B}_{j-1}^k\cdots\mathbf{B}_1^k$, where $\tau_j^{k,i}$ $(i = 1,2,3,4)$ are defined by equation (8). Note that $\mathbf{b}_i$ $(i = 1,3,4)$ are independent of f_j, so $\mathbf{B}(j,k)\mathbf{b}_i = t_i\mathbf{b}_i$ $(i = 1,3,4)$. Let $\tilde{t}_2$ be the forth eigenvalue

of $\mathbf{B}(j,k)$. Since

$$\det(\mathbf{B}(j,k)) = t_1\tilde{t}_2 t_3 t_4$$

and

$$\det(\mathbf{B}(j,k)) = \det(\mathbf{B}_j^k)\cdots\det(\mathbf{B}_j^1) = t_1 t_2 t_3 t_4,$$

$\tilde{t}_2 = t_2$. Thus the eigenvalues of $\mathbf{B}_j^k\mathbf{B}_{j-1}^k\cdots\mathbf{B}_1^k$ are

$$\left\{\tau_j^{k,1}\cdots\tau_1^{k,1}, \tau_j^{k,2}\cdots\tau_1^{k,2}, \tau_j^{k,3}\cdots\tau_1^{k,3}, \tau_j^{k,4}\cdots\tau_1^{k,4}\right\}.$$

Furthermore, since $\lim_{j\to\infty}\tau_j^{k,i}/\lambda_j \le 1/2$, the eigenvalues of $\mathbf{L}_j^k$ are

$$\left\{\frac{\tau_j^{k,1}\cdots\tau_1^{k,1}}{\lambda_j\lambda_{j-1}\cdots\lambda_1}, \frac{\tau_j^{k,2}\cdots\tau_1^{k,2}}{\lambda_j\lambda_{j-1}\cdots\lambda_1}, \frac{\tau_j^{k,3}\cdots\tau_1^{k,3}}{\lambda_j\lambda_{j-1}\cdots\lambda_1}, \frac{\tau_j^{k,4}\cdots\tau_1^{k,4}}{\lambda_j\lambda_{j-1}\cdots\lambda_1}\right\},$$

which tend to 0. □